AD-A096 477 ARMY MISSILE COMMAND REDSTONE ARSENAL AL GROUND EQU--ETC F/G 14/5
A THERMOPLASTIC ACOUSTICAL HOLOGRAPHY RECORDING DEVICE.(U)
SEP 80 D B RIVERS

UNCLASSIFIED DRSMI/RL-81-1-TR SBIE-AD-E950 099 NL

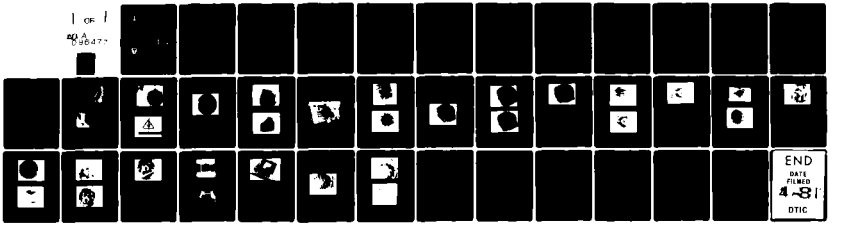

(12) LEVEL III

TECHNICAL REPORT RL-81-1

A THERMOPLASTIC ACOUSTICAL HOLOGRAPHY RECORDING DEVICE

Dr. D. B. Rivers
Ground Equipment and Missile Structures Directorate
US Army Missile Laboratory

25 September 1980

U.S. ARMY MISSILE COMMAND
Redstone Arsenal, Alabama 35898

Approved for public release; distribution unlimited.

DISPOSITION INSTRUCTIONS

DESTROY THIS REPORT WHEN IT IS NO LONGER NEEDED. DO NOT RETURN IT TO THE ORIGINATOR.

DISCLAIMER

THE FINDINGS IN THIS REPORT ARE NOT TO BE CONSTRUED AS AN OFFICIAL DEPARTMENT OF THE ARMY POSITION UNLESS SO DESIGNATED BY OTHER AUTHORIZED DOCUMENTS.

TRADE NAMES

USE OF TRADE NAMES OR MANUFACTURERS IN THIS REPORT DOES NOT CONSTITUTE AN OFFICIAL INDORSEMENT OR APPROVAL OF THE USE OF SUCH COMMERCIAL HARDWARE OR SOFTWARE.

UNCLASSIFIED

SECURITY CLASSIFICATION OF THIS PAGE *(When Data Entered)*

REPORT DOCUMENTATION PAGE		READ INSTRUCTIONS BEFORE COMPLETING FORM
1. REPORT NUMBER RL-81-1	2. GOVT ACCESSION NO. AD-A096	3. RECIPIENT'S CATALOG NUMBER 477
4. TITLE *(and Subtitle)* A Thermoplastic Acoustical Holography Recording Device		5. TYPE OF REPORT & PERIOD COVERED Technical Report
		6. PERFORMING ORG. REPORT NUMBER
7. AUTHOR(s) Dr. D. B. Rivers		8. CONTRACT OR GRANT NUMBER(s) DA1L162303A214
9. PERFORMING ORGANIZATION NAME AND ADDRESS Commander US Army Missile Command ATTN: DRSMI-RL Redstone Arsenal, Alabama 35898		10. PROGRAM ELEMENT, PROJECT, TASK AREA & WORK UNIT NUMBERS AMCMS 6123032140911
11. CONTROLLING OFFICE NAME AND ADDRESS Commander US Army Missile Command ATTN: DRSMI-RPT Redstone Arsenal, Alabama 35898		12. REPORT DATE 25 Sept 1980 13. NUMBER OF PAGES 35
14. MONITORING AGENCY NAME & ADDRESS(if different from Controlling Office)		15. SECURITY CLASS. (of this report) Unclassified
		15a. DECLASSIFICATION/DOWNGRADING SCHEDULE

16. DISTRIBUTION STATEMENT *(of this Report)*

Approved for public release; distribution unlimited.

17. DISTRIBUTION STATEMENT *(of the abstract entered in Block 20, if different from Report)*

18. SUPPLEMENTARY NOTES

This work was accomplished through the Laboratory Research Cooperative Program (LRCP) between Dr. D. B. Rivers of the College of Engineering, University of South Carolina, and the US Army Missile Command.

19. KEY WORDS *(Continue on reverse side if necessary and identify by block number)*

Acoustical holography
Real time
Flaw detection and quantification
Laser and optical reconstruction

20. ABSTRACT *(Continue on reverse side if necessary and identify by block number)*

This report documents an attempt to define the various variables which affect thermoplastic when used as a recorder of ultrasound. Various devices using thermoplastic recording media are illustrated. Specific performance data are given.

DD FORM 1 JAN 73 1473 EDITION OF 1 NOV 65 IS OBSOLETE

SECURITY CLASSIFICATION OF THIS PAGE *(When Data Entered)*

TABLE OF CONTENTS

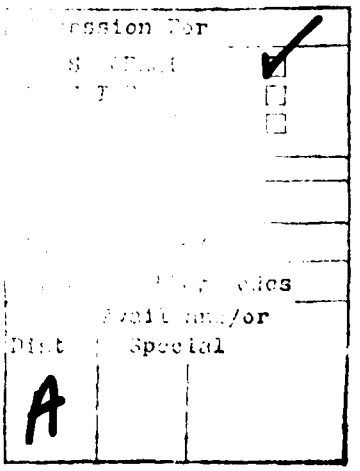

PREFACE

The author wishes to express gratitude for the aid of Drs. W. F. Swinson, W. F. Ranson, D. Smith, H. K. Liu, Mr. J. A. Schaeffel, and Mr. Keith Rodgers.

I. INTRODUCTION

The purpose of this report is to describe the analytical and experimental evaluation of a device to record real-time in situ acoustical holograms. The recording concept investigated, as shown in Figure 1, consists of a layer of thermoplastic (TP) spread over the surface of a rigid substrate.

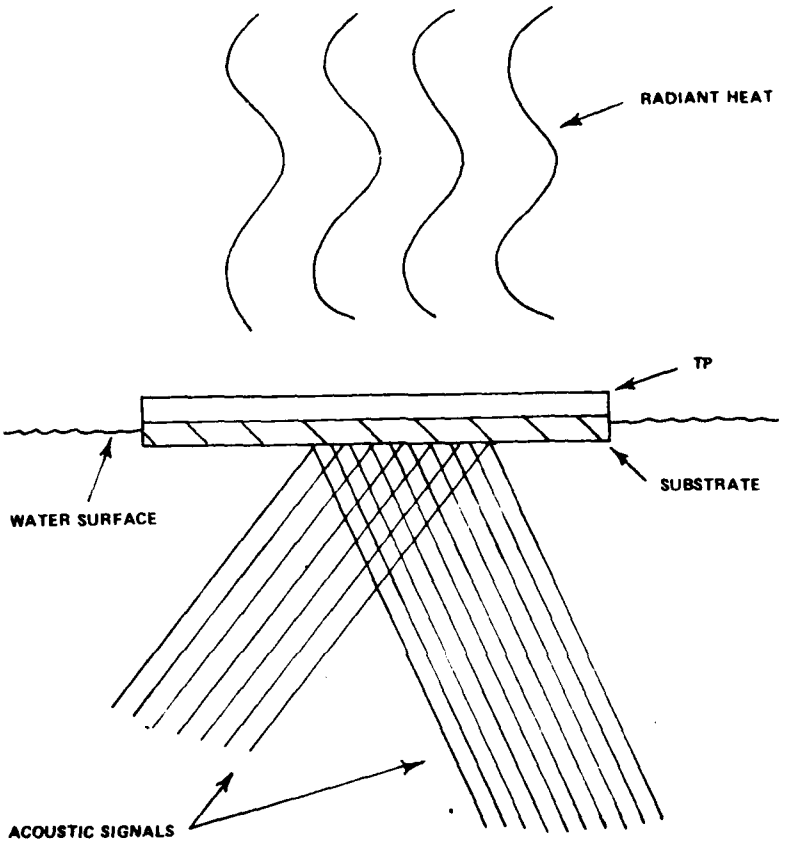

Figure 1. Schematic representation of TP recording device.

This report describes attempts to optimize both substrate and TP. In addition, an effective heating device for the TP is described.

The basic acoustical holography system is shown in Figure 2. It was developed by Irelan, et al. [1] with improvements described by Swinson [2,3]. Additional insight into the problems associated with the TP came from Liu [4].

The use of deformable TP to record optical holograms is well documented in the previously referenced reports. The idea of applying this method to record acoustical holograms was introduced by Young and Wolfe [5] in 1967. Such a technique could have widespread nondestructive testing (NDT) applications where information concerning interior flaws and voids is needed. Of particular interest to the US Army is the application of this method to detect flaws in ceramic radoms and composite materials. There are also potential medical imaging applications for such a device.

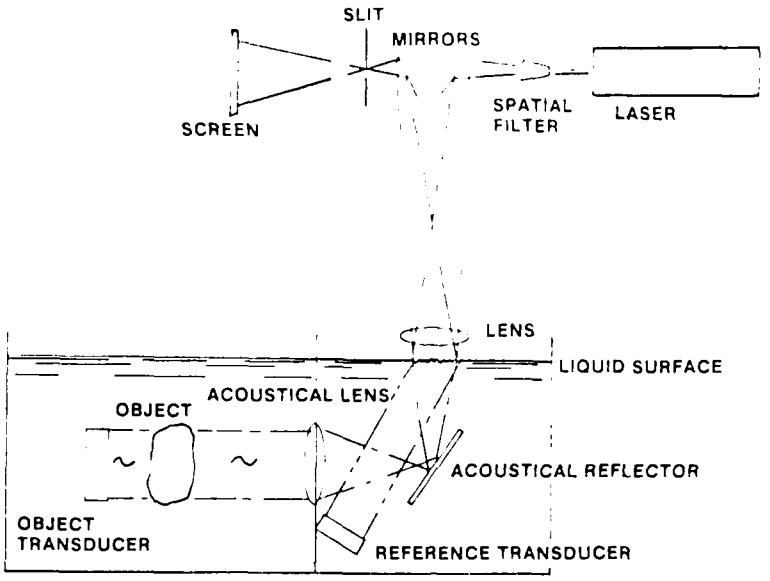

Figure 2. Acoustical holography layout.

II. DISCUSSION OF IDEALIZED SYSTEM

Although there are many possible arrangements and materials which might generate acoustical holographic recordings, this report deals with just one, the arrangement shown in Figures 1 and 2. Ideally, the system would record in situ real-time acoustical holograms as follows.

Two identical underwater collimated ultrasonic beams are focused on the same area of water surface in the imaging tank. One, the object beam, passes through the solid object to be viewed and, therefore, is changed spatially both in amplitude and phase. The second beam, the reference, is unaffected. When both beams combine at the water surface, an interference pattern, the acoustical hologram, is formed by distorting the water surface. Although these acoustical beams are quite powerful, they can only cause microscopic surface distortions due to the weight of the water and its surface tension. However, these distortions are greater than the wavelength of laser light reflected off the water surface, so that a diffraction pattern formed at the focal plane of the light and, by the use of a slit, the zero, first, second, or higher orders of the diffraction orders can be selectively viewed on a screen. The mathematical formulation has been developed by Swinson [3].

To permanently record this interference pattern, some substance other than water must be used since it is obvious that the water levitation will collapse when the ultrasonic signals are removed. This replacement substance must be able to form a liquid surface levitation but be capable of retaining the distortion by some means. The use of TP seems ideal for this application since it is liquid when heated but quickly returns to its solid phase when the heat is removed. The need for a substrate is purely structural.

III. ANALYSIS OF AN IDEAL SUBSTRATE

Before an acoustical wave pattern can be recorded on the TP surface, the waves must first pass through two boundaries: from water to substrate; then from substrate to TP. The following is an analysis and discussion of the energy loss of the ultrasonic waves through these two interfaces.

Consider an incident longitudinal wave of amplitude A_{iL} passing through a liquid-to-solid interface as shown in Figure 3. There are three waves that result:

(1) A reflected longitudinal wave (A_{rL}) back into the liquid,

(2) A transmitted longitudinal wave (A_{tR}) into the solid, and

(3) A transmitted shear wave (A_{tS}) into the solid.

Brekhovskikh [7] has determined that the amplitudes of these three resultant waves can be related to the amplitude of the incident wave by the following ratios:

$$\frac{A_{rL}}{A_{iL}} = \frac{Z_{2L}\cos^2 2\beta + Z_{2S}\sin^2 2\beta - Z_{1L}}{Z_{2L}\cos^2 2\beta + Z_{2s}\sin^2 2\beta + Z_{1L}}, \tag{1}$$

$$\frac{A_{tL}}{A_{iL}} = \frac{\rho_1}{\rho_2} \cdot \frac{2Z_{2L}\cos 2\beta}{Z_{2L}\cos^2 2\beta + Z_{2S}\sin^2 2\beta + Z_{1L}}, \tag{2}$$

and

$$\frac{A_{tS}}{A_{iL}} = \frac{-\rho_1}{\rho_2} \cdot \frac{2Z_{2S}\sin 2\beta}{Z_{2L}\cos^2 2\beta + Z_{2S}\sin^2 2\beta + Z_{1L}}, \tag{3}$$

where the subscripts 1 and 2 represent medium 1 (water) and medium 2 (solid substrate). The acoustical impedances are given by the following:

$$Z_{2L} = \frac{\rho_2 C_{2L}}{\cos \epsilon}, \tag{4}$$

$$Z_{2S} = \frac{\rho_2 C_{2S}}{\cos \beta}, \tag{5}$$

and

$$Z_{1L} = \frac{\rho_1 C_{1L}}{\cos \alpha}, \tag{6}$$

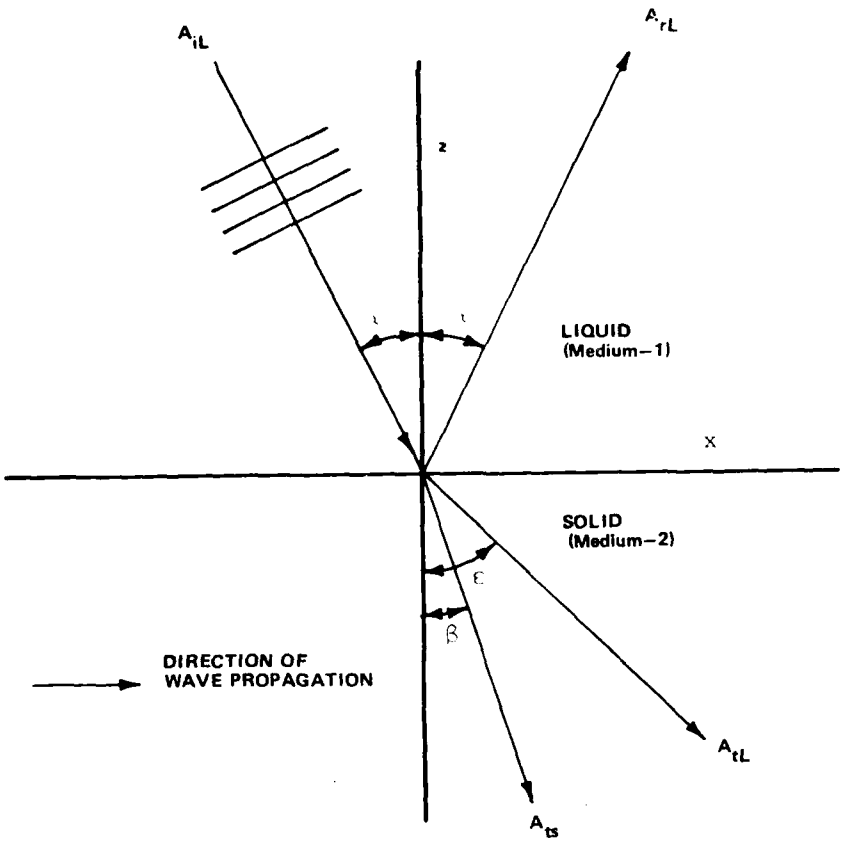

Figure 3. Longitudinal wave propagating from liquid to solid media [6].

where C_{1L} and C_{2L} represent the longitudinal wave propagation velocities in the water and substrate, respectively, and C_{2S} represents the shear wave propagation velocity in the substrate.

To simplify the analysis, it is assumed that the incident longitudinal wave is normal to the water-substrate interface; therefore, $\alpha = 0°$. From Snell's Law applied to acoustics [2],

$$\frac{\sin \alpha}{C_{1L}} = \frac{\sin \beta}{C_{2S}} = \frac{\sin \varepsilon}{C_{2L}} \quad ; \tag{7}$$

therefore, $\alpha = \beta = \varepsilon = 0°$. Using these values, Equations 1-3 can be combined with 4-6 to get the following:

$$\frac{A_{rL}}{A_{iL}} = \frac{\rho_2 C_{2L} - \rho_1 C_{1L}}{\rho_2 C_{2L} + \rho_1 C_{1L}} \quad . \tag{8}$$

$$\frac{A_{tL}}{A_{iL}} = \frac{2\rho_1 C_{1L}}{\rho_2 C_{2L} + \rho_1 C_{1L}} , \tag{9}$$

and

$$\frac{A_{tS}}{A_{iL}} = 0 . \tag{10}$$

The energy contained in an acoustical wave may be expressed as [3]:

$$E_{WAVE} = \frac{\rho_i^2 A_i^2}{Z_i} , \tag{11}$$

where ρ_i, A_i, and Z_i correspond to a shear or longitudinal wave in medium i. Conservation of energy at the interface implies the following:

$$E_{iL} = E_{rL} + E_{tL} + E_{tS} . \tag{12}$$

An ideal substrate would be one which maximizes the amount of transmitted acoustical energy. By combining Equations 9-12, the following expression is obtained and must be maximized:

$$\frac{\text{Energy Transmitted}}{\text{Energy Incident}} = \frac{E_{tL}}{E_{iL}} = \frac{4\rho_1\rho_2 C_{1L} C_{2L}}{\left(\rho_1 C_{1L} + \rho_2 C_{2L}\right)^2} \tag{13}$$

Equation 13 may be considered a function of only two variables, ρ_2 and C_{2L}, since medium 1 will always be water in this experimentation. To maximize this relationship, and hence to discover what values of ρ_2 and C_{2L} would cause maximum acoustical energy transfer from water to substrate, the first partial derivative of the energy ratio with respect to each of the two independent variables is set to zero. Hence,

$$\frac{\partial}{\partial \rho_2}\left[\frac{E_{tL}}{E_{iL}}\right] = 0 . \tag{14}$$

and

$$\frac{\partial}{\partial C_{2L}}\left[\frac{E_{tL}}{E_{iL}}\right] = 0 . \tag{15}$$

Both Equations 14 and 15 yield identical solutions of

$$\rho_2 C_{2L} = \rho_1 C_{1L} . \tag{16}$$

To determine if Equation 16 represents a maximum or minimum, the second derivative test is applied to the solutions of Equations 14 and 15. That is, for Equation 14,

$$\left[\frac{\partial^2}{\partial \rho_2^2}\left(\frac{E_{tL}}{E_{iL}}\right)\right]_{\rho_2 = \frac{\rho_1 C_{1L}}{C_{2L}}} < 0 \qquad (17)$$

and

$$\left\{\left[\frac{\partial^2}{\partial \rho_2^2}\left(\frac{E_{tL}}{E_{iL}}\right)\right]\left[\frac{\partial^2}{\partial C_{2L}^2}\left(\frac{E_{tL}}{E_{iL}}\right)\right] - \left[\frac{\partial^2}{\partial \rho_2 \partial C_{2L}}\left(\frac{E_{tL}}{E_{iL}}\right)\right]\right\}_{\rho_2 = \frac{\rho_1 C_{1L}}{C_{2L}}} > 0 \quad . \qquad (18)$$

The solution to Equation 15 must satisfy

$$\left[\frac{\partial^2}{\partial C_{2L}^2}\left(\frac{E_{tL}}{E_{iL}}\right)\right]_{C_{2L} = \frac{\rho_1 C_{1L}}{\rho_2}} < 0 \qquad (19)$$

and

$$\left\{\left[\frac{\partial^2}{\partial^2 C_{2L}}\left(\frac{E_{tL}}{E_{iL}}\right)\right]\left[\frac{\partial^2}{\partial^2 \rho_2}\left(\frac{E_{tL}}{E_{iL}}\right)\right] - \left[\frac{\partial^2}{\partial C_{2L} \partial \rho_2}\left(\frac{E_{tL}}{E_{iL}}\right)\right]\right\}_{C_{2L} = \frac{\rho_1 C_{1L}}{\rho_2}} > 0 \quad . \qquad (20)$$

The solutions to Equations 17 and 19 are, respectively,

$$-0.5\left(\frac{C_{2L}^2}{\rho_1^2 C_{1L}^2}\right) \text{ and } -0.5\left(\frac{\rho_2^2}{\rho_1^2 C_{1L}^2}\right) \quad , \qquad (21)$$

both of which are always negative. Evaluation of Equations 18 and 20, however, both yield results equal to zero. Hence, it cannot be confirmed yet that satisfying result (Equation 16) will yield maximization of the energy transfer.

By substituting result (Equation 16) into Equation 13, the following is shown

$$\frac{E_{tL}}{E_{iL}} = 1.0 \quad . \tag{22}$$

This result, when combined with the zero evaluation of Equations 18 and 20, implies that there are an infinite number of values of ρ_2 and C_{2L} which will maximize the energy transfer into the substrate. All that is required is that condition in Equation 16 be met. In other words, for best energy transfer, an acoustic characteristic impedance match is required. This same type of reasoning can also be applied to the substrate - TP interface. It is complicated by the fact that, as explained later, the TP lower surface is approximately equal to the water tank temperature (typically 22°C) while the TP upper surface is heated to improve its recording characteristics. Therefore, the velocity of longitudinal waves in the TP changes as the phase of the TP changes from a solid to a liquid state. Table 1 shows impedances of water and several potential substrates.

TABLE 1. CHARACTERISTIC IMPEDANCES OF VARIOUS MATERIALS

MATERIAL	DENSITY (ρ) g/cm^3	VELOCITY (C_L) cm/s	ρC_L
Water	1.0	1.45×10^5	1.45×10^5
Plexiglass	1.18	2.68×10^5	3.2×10^5
Plate Glass	2.51	5.77×10^5	15.4×10^5
Pyrex	2.23	5.57×10^5	12.4×10^5
Teflon	2.2	1.35×10^5	3.0×10^5
Nylon	1.20	2.0×10^5	2.40×10^5
Aluminum	2.7	6.4×10^5	17.3×10^5
Steel	7.8	6×10^5	46.8×10^5

IV. EXPERIMENTATION AND DISCUSSION

A. Initial Recordings

An initial attempt to record an acoustical wave pattern on TP was performed. Figure 4 shows the test fixture, a plexiglass base plate with 114.3-mm square interior wall to contain the TP, and a high outer wall to keep any water from the imaging tank out of the test fixture. The three leveling screws and the two bubble levels were added later to aid in the positioning of the test fixture on the water surface. Figure 5 shows the initial TP recording made with this device. Only the 3 MHz reference transducer was activated. The 3 MHz object transducer was not activated. The TP was S-25. This particular TP was sufficiently fluid at room temperature so that additional heating was not necessary for image formation. The concentric

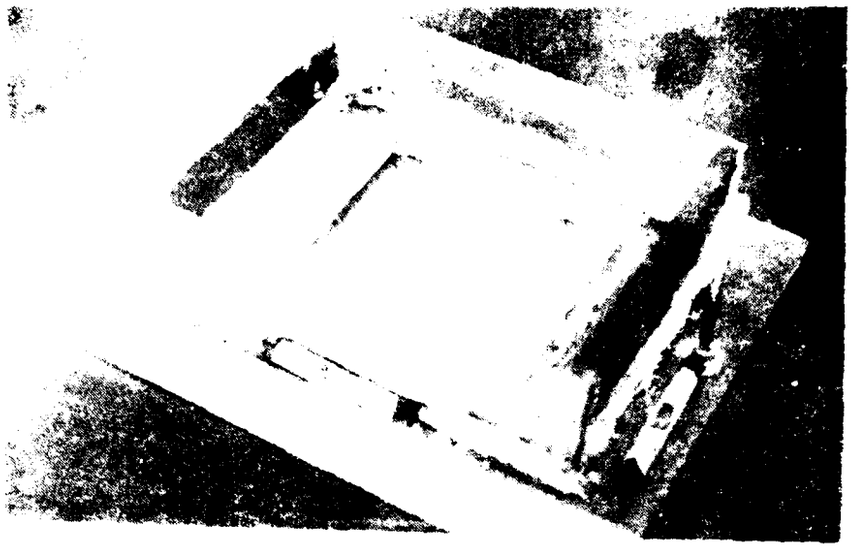

Figure 4. Holographic recording setup with square fresnel window.

Figure 5. TP recording of fresnel zone acoustical ring pattern from 3-MHz reference transducer, (acoustic signal on).

pattern of the fresnel zone rings is clearly visible. Figure 6 shows the same image one minute after the reference beam was turned off. Although there is no apparent difference in these two photographs, it should be noted that the ring pattern faded significantly after two minutes and was completely gone at the end of five minutes. This image fading was caused by the S-2A TP being too fluid at room temperature and indicated that TP with a higher melting temperature would be needed for permanent recordings.

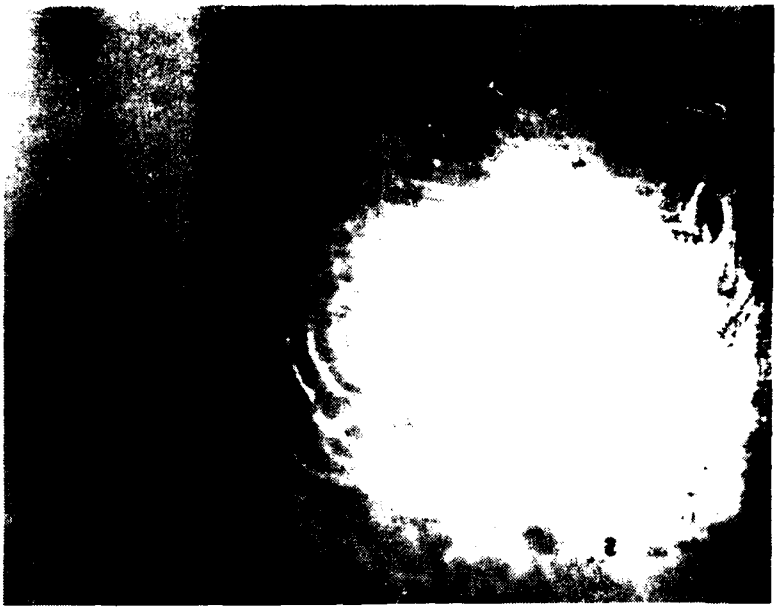

Figure 6. TP recording of fresnel zone acoustical ring pattern from 3-MHz reference transducer (one minute after removal of acoustic signal).

Potential problems with higher temperature TP are shown with the following four figures. Figure 7 is the target object used for acoustical imaging in

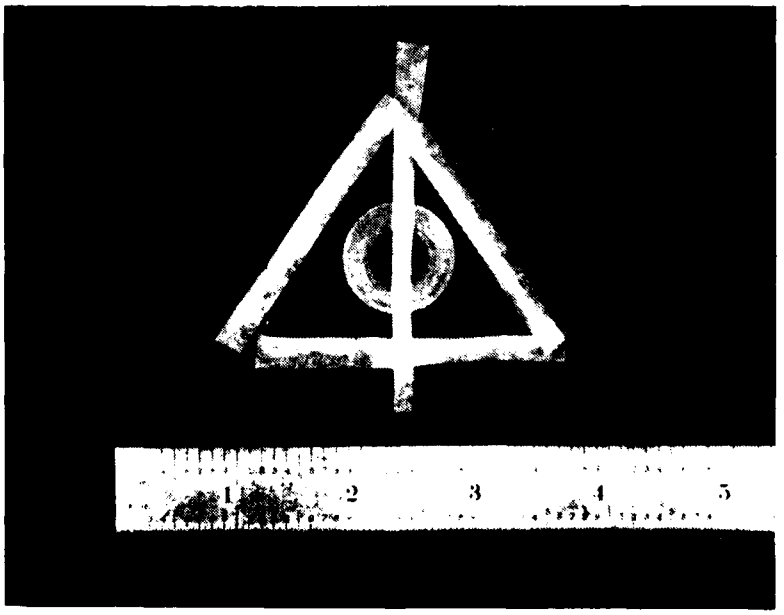

Figure 7. Acoustical target.

the remainder of the experiments in this report. A flat washer was taped to a 12.7-mm thick sheet of plexiglass. The washer was surrounded by a taped triangle. Since the tape was not expected to image well, a thin strip of metal foil lined the underside of the tape. The target was located in the imaging tank according to Figure 2. To get an idea of what kind of TP image to expect, a water surface image was first produced by filling the 114.3-mm square in the recording device with a 6.35-mm layer of water instead of TP, as shown in Figure 8. Only the object beam was activated. The black dots

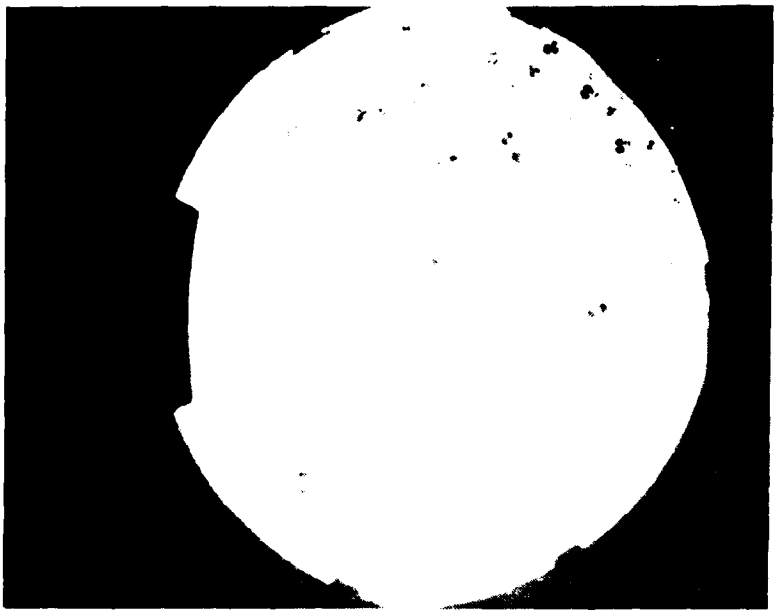

Figure 8. Water surface image of object target using water layer instead of TP in recording fixture with square window (object beam only).

superimposed on the image were caused by dust floating on the water surface and water drops on the underside of a focusing lens directly above the water surface. The water in the square window recorder was then removed and replaced with a 2.54-mm layer of S-25 TP previously heated to 120°C. This high temperature was needed to lower the TP viscosity sufficiently so the TP would easily flow and form an even surface across the bottom of the recording device. Previous experimentation had shown that S-25 TP needed to be heated to at least 90°C so that air bubbles caused by pouring the TP would not be trapped in the liquid. The heat from the melted TP caused the 1.524-mm thick plexiglass base of the recording device to warp. Consequently, it was difficult to align the recording device so that a flat recording area could be found. Figure 9 shows the unevenness of the upper surface of the TP prior to activation of the object transducer. This unevenness of the recording TP distorted the acoustical image when the object beam was activated as shown in Figure 10. However, this recorded image was still superior to any previous attempts and the object target was clearly visible. It also faded approximately five minutes after removal of the acoustic beam.

Figure 9. Uneven TP surface in square window recording device before acoustical signal was applied.

Figure 10. TP recording of imaging target on square window recording device (object beam only).

An attempt was made to further enhance the image shown in Figure 10 by heating the TP surface. The heating device consisted of a 1.27 x 1[illegible] glass plate laid over the 114.3-mm square borders of the recording device. The bottom side of the glass was coated with ITO, a transparent but resistive material. Several different methods were used to attach electrodes to opposite sides of the glass plate so that the glass would not break due to thermal expansion differences between the glass and the electrodes. However, even after this electrode problem was solved, it was found that the coated glass could not generate sufficient heat to change the temperature of the TP before the glass broke from excessive temperature. This might have been corrected by using coated pyrex, but such was not available. A different type of heater is discussed later in this report.

To better isolate the recording fixture from ripples in the imaging tank, the fixture was suspended from two metal straps above the water surface by three leveling screws, as shown in Figure 11. In addition, the fixture was

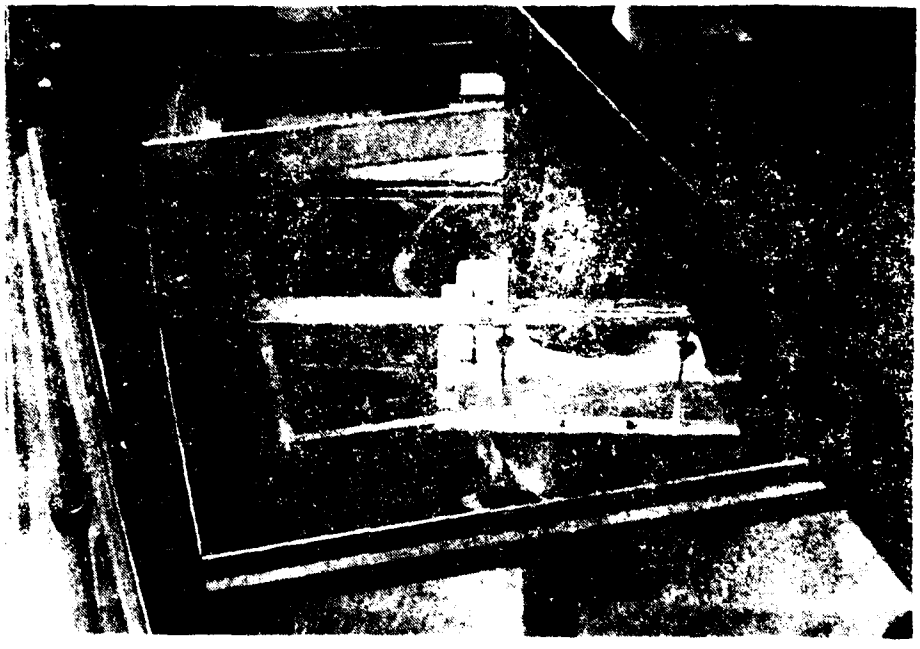

Figure 11. Recording fixture suspended by leveling screws in the imaging tank.

allowed to sit in the tank for one day so that gravity could level the surface as much as possible. Figure 12 shows the new S-[illegible] TP. The fixture base was 1.524-mm thick topped with a 2.108?-mm layer of [illegible] the object beam was activated. Figure 13 shows the image after the heater was activated for 20 minutes. Again it can be seen that the enhancement of the image came from the low heat level of the glass [illegible].

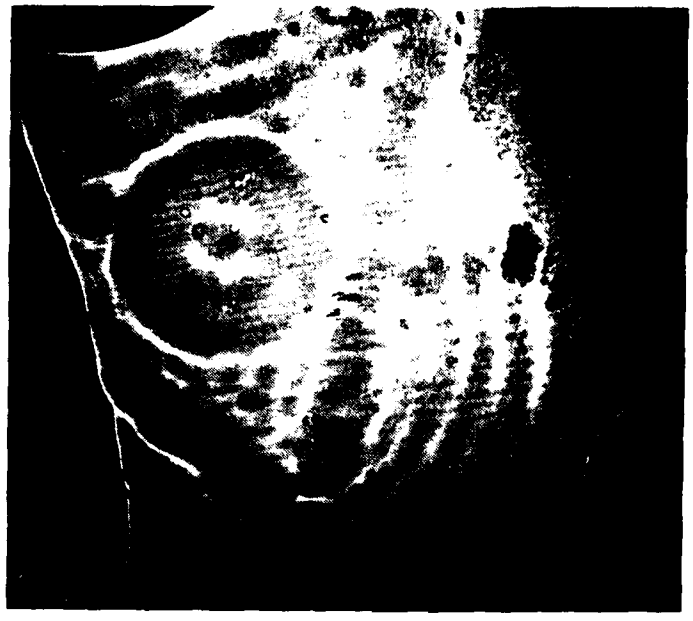

Figure 12. Improved TP recording (object beam only).

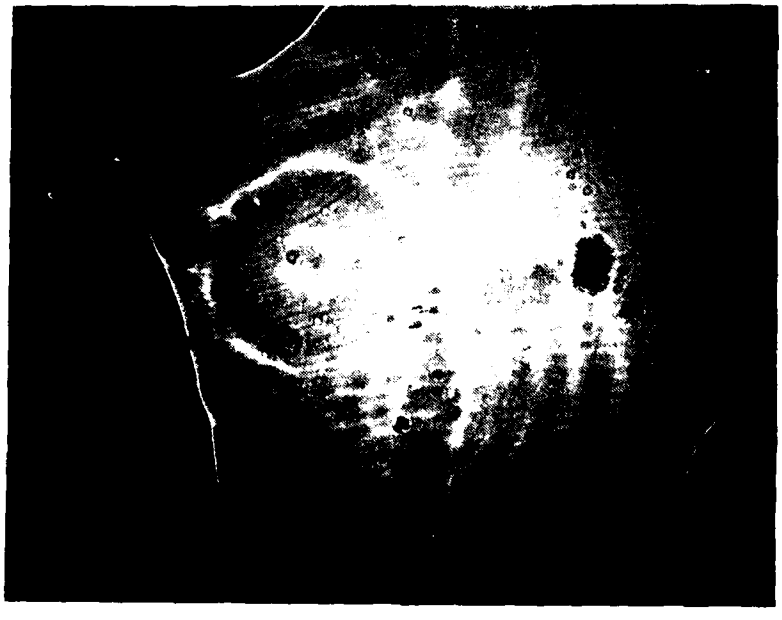

Figure 13. TP recording after 25 minutes exposure to heat (object beam only).

B. Effect of Substrate Thickness

Since the 1.524-mm thick plexiglass base of the recording device was not capable of maintaining the required flatness after the liquified TP was poured due to thermal warping, a study was undertaken to determine how much image quality would be lost by using a thicker plexiglass base. The recording device was modified so that the base area inside the 11.43-cm square was removed. Plexiglass squares of various thicknesses were then temporarily attached to the underside of the device and a 6.35-mm water layer was used as an imaging medium instead of TP. Figures 14 through 17 show the deterioration of the water surface image caused by increasingly thick plexiglass bases, from no base at all up to 6.35-mm. Only the object transducer was activated. Besides having a poorer image due to greater ultrasound energy losses inside the plexiglass from internal relaxation absorption and attenuation, the 6.35-mm plexiglass also warped when heated with a heat lamp in an attempt to liquefy a TP layer.

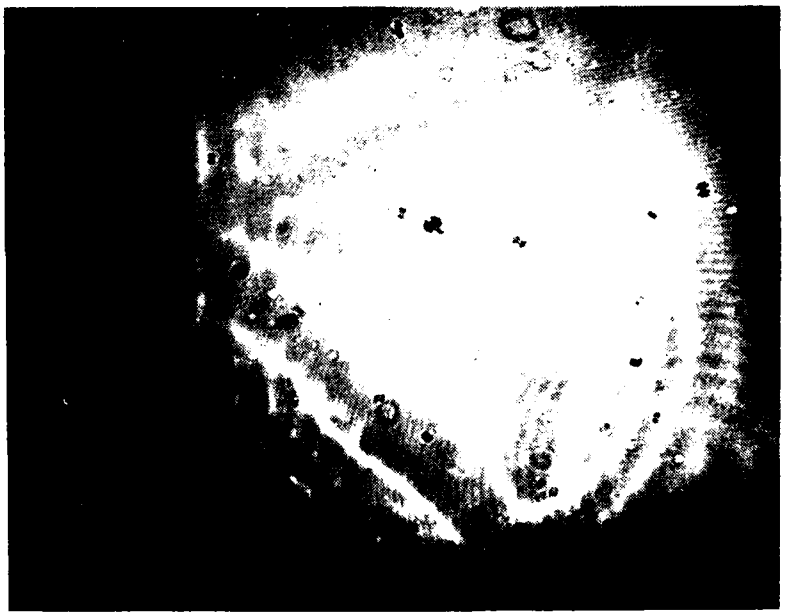

Figure 14. Water surface image with no substrate.

To find a more heat resistant substrate, the water imaging experiment was repeated using both mylar and glass. The .0889-mm mylar deformed significantly, not from the heat but from the water pressure on its lower side when the recording fixture was placed in the imaging tank, even though the mylar was positioned less than 6.35-mm below the tank water surface. This indicated that rigidity of the substrate was also a desirable quality. A 1.320-mm thick glass plate was sufficiently rigid but, as analytically proven in Section III, the glass reflected most of the ultrasound so that insufficient energy was available to form a water surface image.

Figure 15. Water surface image with 1.650-mm thick plexiglass substrate.

Figure 16. Water surface image with 3.225-mm thick plexiglass substrate.

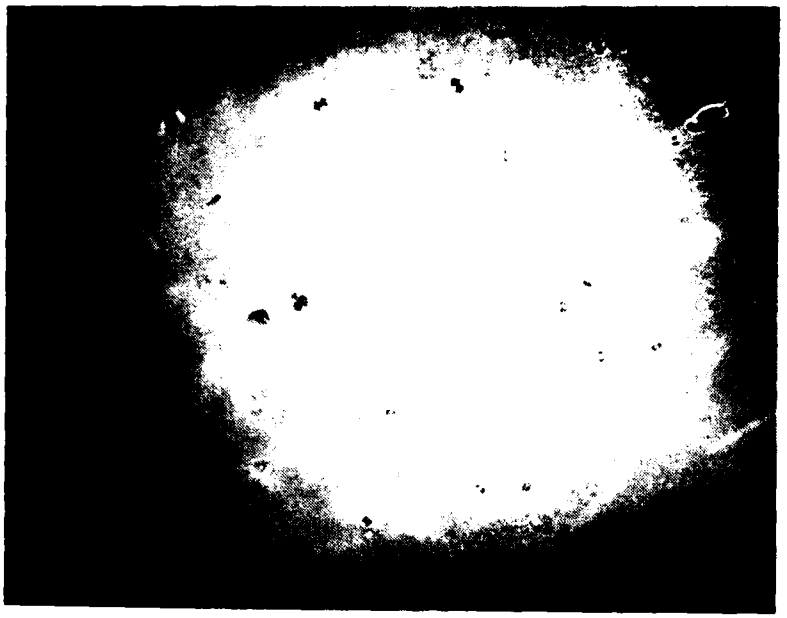

Figure 17. Water surface image with 6.35-mm thick plexiglass substrate.

C. Effect of TP Surface Smoothness

Up to this point, all images were recorded with only one acoustical transducer activated. By activating both transducers, an acoustical hologram can be generated at the liquid surface, although there is some argument that the images already shown were Gabor in-line holograms. Nevertheless, by activating both transducers, a true interference pattern is formed. This interference image, when viewed at the optical focal plane, produces a bright dot which represents the zero order diffraction and a series of diffraction lines above and below the central dot which represent the first, second, and higher diffraction views as mathematically shown by Swinson [3]. Figures 18 through 20 show the zero, first, and second order diffraction images discretely. As can be seen, the contrast is significantly improved by viewing the target at higher diffraction views. These water surface images were recorded at increasing laser power to compensate for the decreasing brightness of each successively higher diffraction order.

To create similar diffraction images on a TP layer, the surface of the TP was required to be optically flat. All attempts to record diffraction patterns on the TP were unsuccessful due to a lack of flatness which prevented the reflected light from forming a spot on the optical focal plane. Instead, an unfocused folded image was created at the focal plane, making it impossible to separate diffraction orders. This uneven upper TP surface was caused by a combination of several separate problems. Besides the rigidity question which has already been raised, the surface of the TP formed a convex meniscus after pouring. This tended to expand the reflected light beam and destroy the potential for separating diffraction orders at the focal plane. Of course, as the distance from the boundaries increased, the surface

Figure 18. Zero order water surface hologram.

Figure 19. Zero order water surface hologram.

Figure 20. Second order water surface hologram.

more closely approximated a flat surface. In fact, a previous experiment had shown that water in the 114.3-mm square recording device formed a less than flat surface due to meniscus curvature and this made separation of diffractions more difficult. By filling the recording device with enough water to cover the 114.3-mm square retaining walls, thereby causing the outer walls to become retaining walls, the boundary effects were sufficiently remote from the central recording area and a normal diffraction pattern was observed at the focal plane.

A new recording device was designed in a further attempt to create a flat TP recording surface. As shown in Figure 21, the new device differed from the old in several ways. The plexiglass base was replaced with 6.35-mm thick aluminum for rigidity. The 114.3-mm square central acoustical opening was replaced by a 76.2-mm diameter round hole to maximize the rigidity of the substrate insert. A 76.2-mm diameter window was the smallest acoustical window thought practical and the round shape of an acoustical substrate insert minimized deflections due to underside water pressure. The interior retaining walls were removed so that the outer walls acted as a retaining wall for the TP and a water barrier as well, thereby causing the TP to approximate a flat surface near the central acoustical window since this window was far removed from the boundary effects.

D. Effect of Substrate Surface Roughness

Plugs (76.2 mm in dia.) of various substrate materials were placed in these new recording devices. Water surface holograms were taken to compare these materials. Figures 22 and 23 show the zero and first order diffraction images through a 3.860-mm thick nylon substrate plug covered with 12.7-mm of water. The quality of the images was significantly below that of the water surface holograms with no substrate due to the relaxation absorption and

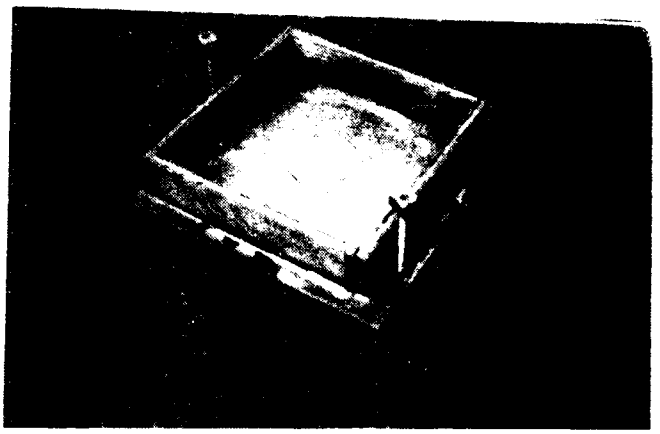

Figure 21. Improved recording device.

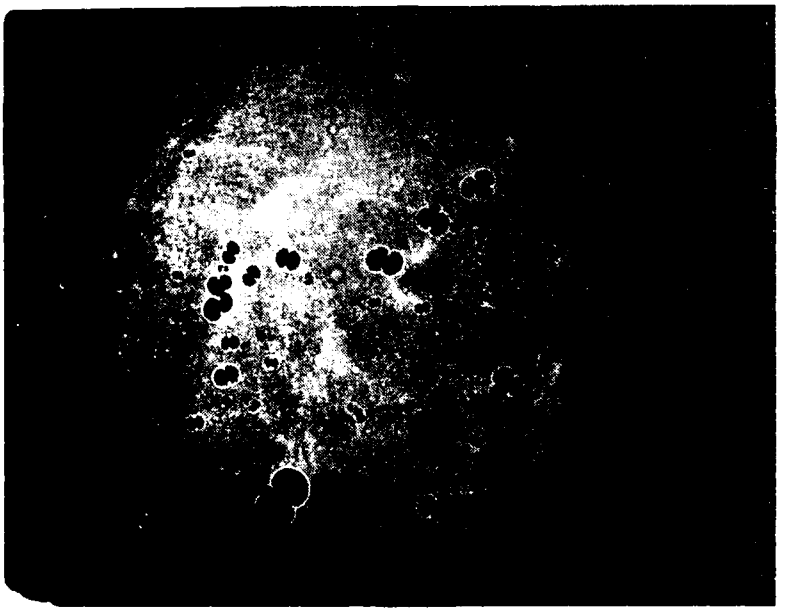

Figure 22. Zero-order water surface [illegible]
[illegible] 6.35-mm thick nylon substrate.

Figure 23. First order water surface acoustical hologram through 3.860-mm thick nylon substrate.

attenuation of the ultrasound through the substrate material. Figures 24 and 25 show the zero and first order images through a similar nylon plug which had been sanded to a thickness of 1.778-mm. In comparing these with the two previous illustrations, it can be seen that no real improvement of the images resulted, even though the substrate thickness had been more than halved. In fact, there was some deterioration of image quality in the first order images.

It was theorized that substrate surface roughness might account for these results, since the thinner nylon plug had a rougher surface caused by the sanding. The wavelength of 3-MHz ultrasound in water is 0.508-mm. Sanding the nylon plug with 100-count sandpaper might have caused surface variations in the substrate of the same order of magnitude as the wavelength of the ultrasound, thereby causing the image to distort. To test this theory, the thicker nylon plug was sanded with 100-count paper until rough and another first order water surface holograph was attempted. The image quality was greatly reduced as shown in Figure 26. In a further test the surfaces of the thinner nylon plug were sanded with increasingly fine sandpaper up to 600 count. The surfaces were then polished with a polishing compound and a first order hologram was imaged, as shown in Figure 27. Some improvement in the image can be seen, indicating that an ideal substrate should have acoustically smooth surfaces.

Figure 28 shows a first order hologram of a 1.600-mm thick teflon substrate plug. This image was clearly superior to any previously generated, although the teflon surface was not particularly flat. This indicated that teflon had a lower degree of attenuation and relaxation absorption than other materials investigated.

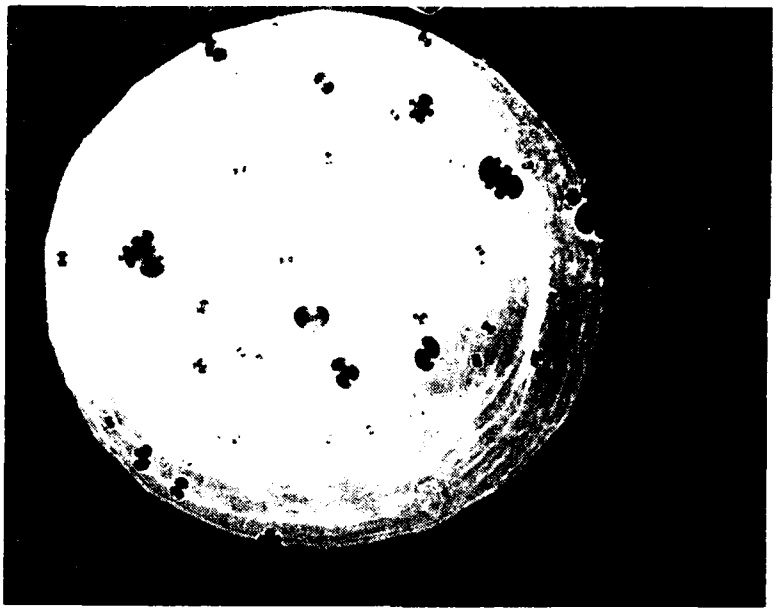

Figure 24. Zero order water surface acoustical hologram through 1.778-mm thick nylon substrate.

Figure 25. First order water surface acoustical hologram through 1.778-mm thick nylon substrate.

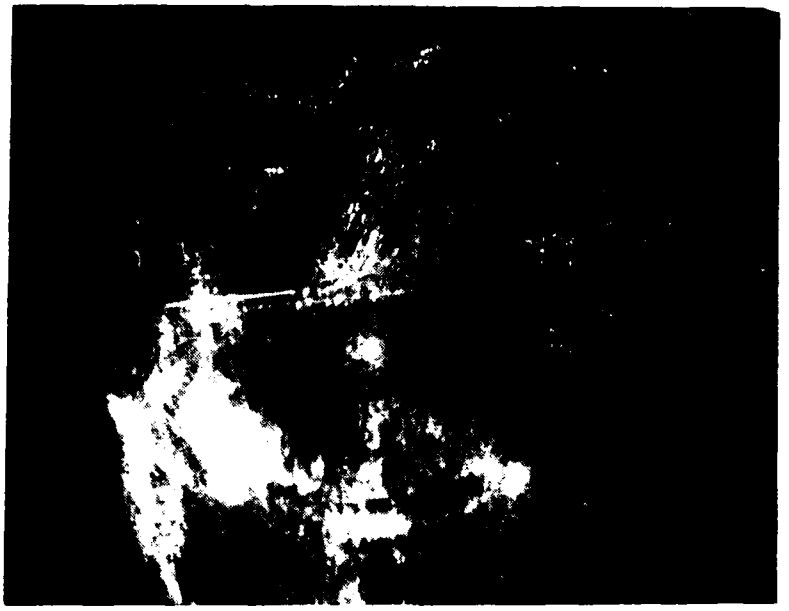

Figure 26. First order water surface acoustical hologram through 3.860-mm thick nylon substrate (sanded rough).

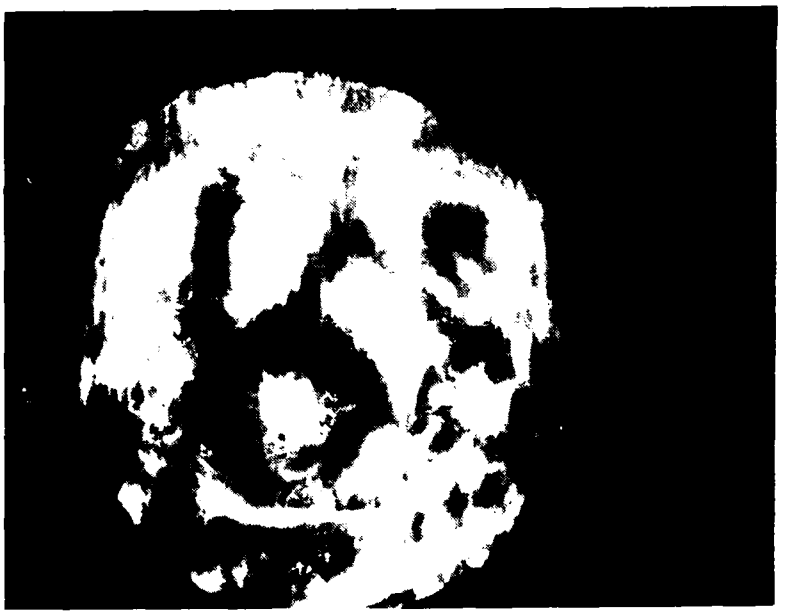

Figure 27. First order water surface acoustical hologram through 1.778-mm thick nylon substrate (polished).

Figure 28. First order water surface acoustical hologram through 1.600-mm thick teflon substrate.

E. Heating Device

A device was designed and constructed to heat high melting point TP to a liquid for image formation. As seen in Figures 29 and 30, the device consisted of a plywood top with a central opening for the spatially filtered laser beam. Thin (0.254-mm dia.) stainless steel wire was wound between two sets of hooks, which were attached to spring loaded movable supports. Heat was generated by passing an AC current from a variable transformer through the resistive device (57 ohms cold). As the wire heated, significant thermal expansion occurred, but this was compensated for by the expansion of the springs on each movable support, thus keeping the wires taut. Experimentation showed that 160V could be tolerated by this device before the wires broke (500W). Figure 31 shows the heating device installed in the recording fixture. The construction of the heater is such that the wires are positioned approximately 6.35-mm above the TP layer. Figure 11 shows the entire assembly installed in the imaging tank.

F. Additional TP Recordings

The round window recording device was prepared for TP recording. The substrate plug used was Teflon, since it had previously produced the best water images. The plug was attached to the aluminum base of the recorder with silicon rubber so that the Teflon upper surface was level with the aluminum upper surface. Small gaps between the edges of the two materials were filled with automotive body putty so that the smoothest possible continuous surface could be achieved. The recorder base was then coated with 2.54-mm thick layer of S-55 TP, a material which is rigid at room temperature. The TP had to be heated to 125°C before pouring in order for it to flow to an

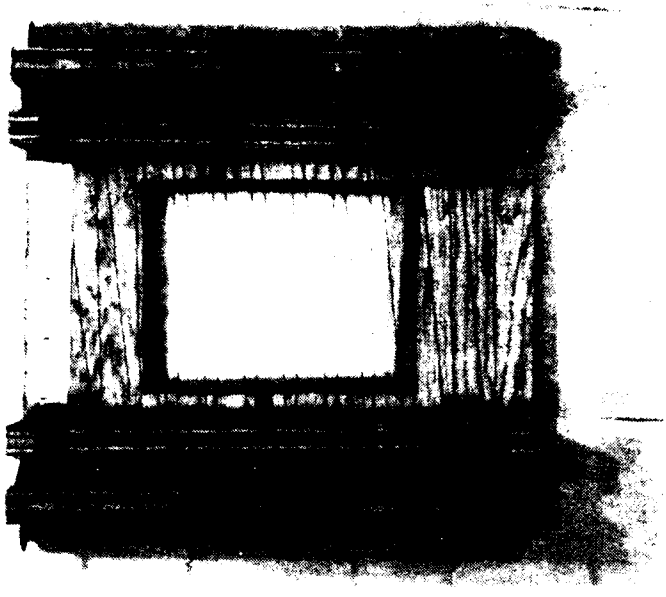

Figure 29. Bottom view of new heating device.

Figure 30. Side view of new heating device.

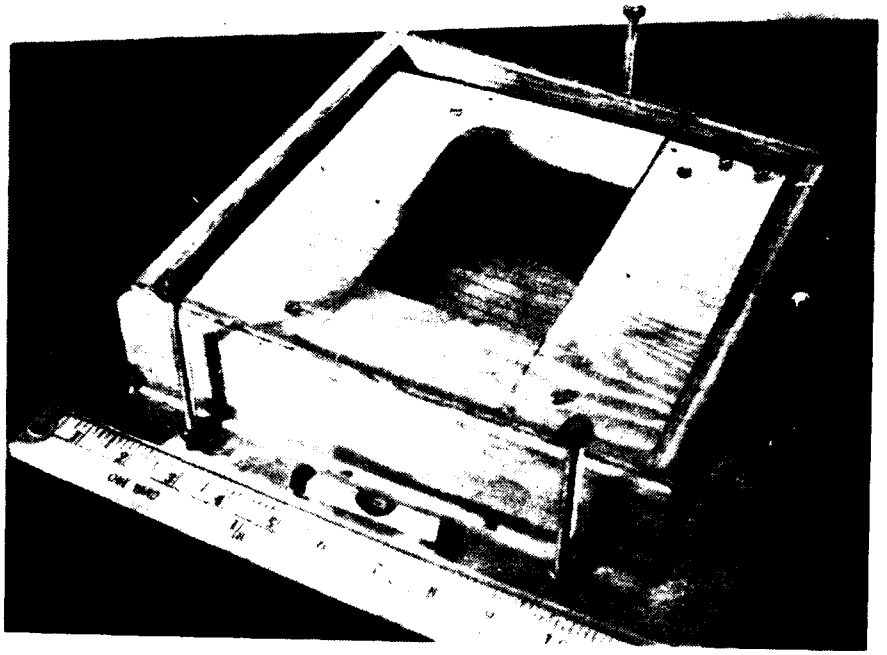

Figure 31. Heating device in recording fixture.

even layer on the recorder. The heating device was then installed. The assembly was first tested with no acoustic signals to verify that the TP would adequately liquify with the heater activated. This test was necessary since it was not known whether or not the effect of having the bottom of the TP coupled through a heat conducting medium (the aluminum base or the thin substrate) to a heat sink (the tank water). One could assume that the TP would be in a multiple phase during heating since the top would liquify from the radiant heat but the bottom might always remain close to the temperature of the tank water and not liquify. The test showed that the TP liquified completely. However, the square viewing hole had to be covered with another wood block so that enough heat could be retained in the vicinity of the TP for proper liquification. This did not, as one might assume, destroy the possibility of in situ real-time recording. However, previous experimentation had shown that the laser light image was temporarily distorted when the heater was activated due to air convection currents. These distortions disappeared immediately when the heater was deactivated. By modifying the heater so that the central window was permanently covered with optical grade pyrex, one could use the heater without adding and removing a heat retaining cover.

When the heat was removed, it was observed that the TP surface was slightly distorted around the perimeter of the substrate disk. Although great care had to be taken to insure a smooth continuum between aluminum base and substrate disk, there were still slight depth variations. When the TP was liquified or when water was used as an imaging medium no upper surface imperfections existed since the shear forces caused by these depth variations could not be transmitted from the bottom of a liquid imaging media to the top. Consequently, the top of these liquids always was plane. However, as the TP

cooled when the heater was deactivated, the TP crystal from a pure liquid phase toward a solid phase. During this ambient period, the TP could, and in fact did, transmit these imperfections to the top TP surface so that a slight boundary effect was evident all around the substrate plug on the TP surface. This meant that higher order diffraction views could not be generated due to a nonplane imaging surface on the TP. However, zero order views of the target were generated as seen in Figures 32 through 34. This three-photo sequence demonstrated an interesting property of TP which bears additional study. As can be seen, the images are slightly distorted, especially the heating wires, since the reflecting TP surface was not adequately plane. However, as the TP cooled the images grew in size. This appears to be caused by a slight curvature change of the TP surface, so that the curvature increased as the TP cooled, thereby causing a lens-like expansion of the light image. Whether or not this effect would be present had the TP surface originally been plane is not obvious.

Figure 32. S-55 TP zero order image one minute after removal of heat.

V. CONCLUSIONS AND RECOMMENDATIONS

The results of the investigation are summarized as follows. Analysis of the transmission-reflection properties between water and substrate showed that a characteristic impedance match was necessary to transmit the maximum acoustic energy into the substrate TP complex. Materials such as Teflon, nylon, Mylar, and plexiglass were shown to be relatively transparent to ultrasound. The heat required to liquify the TP necessitated that the substrate be resistant to thermal deformation up to 125°C. Of the above group, all but plexiglass were satisfactory. The substrate should have minimum relaxation absorption and attenuation properties so that the maximum acoustic

Figure 33. S-55 TP zero order image five minutes after removal of heat.

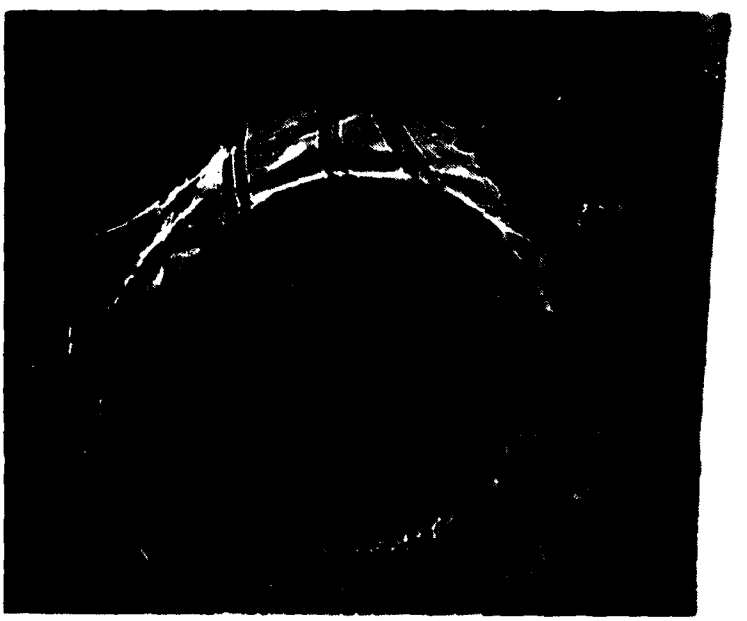

Figure 34. S-55 TP zero order image thirty minutes after removal of heat.

energy might be transmitted to the TP. For a similar reason, the substrate should be as thin as possible. However, the thinner a given substrate, the less rigid. Experimentation showed that slight surface deformation caused by water pressure and TP weight had a severe impact on the ability of the recorder to reproduce diffraction order views. The recorded image was also subject to distortion if the substrate and TP surfaces where not acoustically pure; i.e., if the surface roughness was not at least an order of magnitude below the wavelength of the ultrasound.

The TP layer needed to be no thicker than that necessary to free the central recording area from boundary effect distortions. Thickness of TP above this caused a lessening of the visual image since the TP itself exhibits significant relaxation absorption and attenuation of ultrasonic signals. The type of TP used was shown to be a trade-off between a sufficiently high melting point (so that the TP was rigid at room temperature) and some maximum temperature (dependent on the substrate) so that the substrate would not thermally deform when the TP was heated to a liquid during holographic recording.

Recommendations for system modification include the following. Smaller diameter transducers of higher power would enhance the images by allowing the system to operate in the "cleaner" Fraunhofer zone as opposed to the fresnel zone, where the large diameter transducers currently being used operate. The additional power would also allow the use of a substrate with a poorer characteristic impedance match but greater rigidity. Therefore, a recording fixture with a separate acoustical window would not be necessary so that no localized substrate boundary effects would affect the TP surface smoothness. Thus, the TP would be able to record and reproduce the higher order diffraction images. In addition, higher power transducers would allow the use of a higher frequency ultrasonic signal, which would improve the resolution of the system.

In addition, the use of thin film (thickness 0.254-mm) TP should be investigated. Although this has been tried previously without applying a sufficiently smooth and level coating of TP, the technology does exist to perform this coating successfully.

The effect of TP surface modification during cooling should also be investigated, since failure of the TP to retain the acoustical interference pattern correctly would obviously eliminate it from consideration as a recording medium.

REFERENCES

1. Irelan, V. G., B. R. Mullinix, J. G. Castle, "Real-Time Acoustical Holography Systems," US Army Missile Research and Development Command, Technical Report T-78-10, Redstone Arsenal, AL, October 1977.

2. Swinson, W. F., "Optimizing a Real-Time Acoustical Holography System," US Army Missile Command, Technical Report RL-80-2, Redstone Arsenal, AL, 1 October 1979.

3. Swinson, W. F., "Improving a Real-Time Acoustical Holographic System for Flaw Detection," US Army Missile Command, Technical Report RL-80-3, Redstone Arsenal, AL, 35809, 1 October 1979.

4. Liu, H. K., "A Thermoplastic Device for Real-Time In-Situ Recording of Acoustical Holograms," US Army Missile Command, Technical Report RL-80-4, Redstone Arsenal, AL, 1 October 1979.

5. Young, J. D., J. E. Wolfe, "A New Recording Technique for Acoustical Holography," Applied Physics Letters, Vol. 11 (1967), p. 294.

6. Schaeffel, J. A., Jr., "Acoustical Speckle Interferometry," Technical Report T-79-39, US Army Missile Research and Development Command, Redstone Arsenal, AL, March 1979.

7. Brekhovskikh, L. M., Waves In Layered Media, Academic Press, New York, 1960.

8. Hildebrand, B. P., B. B. Brenden, An Introduction to Acoustical Holography, Plenum Press, 1972.

DISTRIBUTION

	No. of Copies
Director USA Mobility Equipment Research and Development Center Coating and Chemical Laboratory ATTN: STSFB-CL Aberdeen Proving Ground, MD 21005	1
Commander Edgewood Arsenal ATTN: SAREA-TS-A Aberdeen Proving Ground, MD 21010	1
Commander Picatinny Arsenal ATTN: SARPA-TS-S, Mr. M. Costello Dover, NJ 07801	1
Commander Rock Island Arsenal Research and Development ATTN: 9320 Rock Island, IL 61201	1
Commander Watervliet Arsenal Watervliet, NY 12189	1
Commander US Army Aviation Systems Command ATTN: DRSAV-EE -MT, Mr. Vollmer St. Louis, MO 63166	1 1
Commander US Army Aeronautical Depot Maintenance Center (Mail Stop) Corpus Christi, TX 78403	1
Commander US Army Test and Evaluation Command ATTN: DRSTE-RA Aberdeen Proving Ground, MD 21005	1
Commander ATTN: STEAP-MT Aberdeen Proving Ground, MD 21005	1

Technical Library
Naval Ordnance Station
Indian Head, MD 20640 — 1

Commander
US Army Materiel Development and Readiness Command
ATTN: DRCMT — 1
Washington, DC 20315

Headquarters
SAC/NRI (Stinfo Library) — 1
Offutt Air Force Base, NE 68113

Commander
Rock Island Arsenal
ATTN: SARRI-KLPL-Technical Library — 1
Rock Island, IL 61201

Commander (Code 233)
Naval Weapons Center
ATTN: Library Division — 1
China Lake, CA 93555

Department of the Army
US Army Research Office
ATTN: Information Processing Office — 1
P. O. Box 12211
Research Triangle Park, NC 27709

Commander
US Army Research Office
ATTN: DRXRO-PW, Dr. R. Lontz — 2
P. O. Box 12211
Research Triangle Park, NC 27709

US Army Research and Standardization Group (Europe)
ATTN: DRXSN-E-RX, Dr. Alfred K. Nodoluha — 2
Box 65
FPO New York 09510

Headquarters
Department of the Army Office of the DCS for Research
Development and Acquisition
Room 3A474, The Pentagon
ATTN: DAMA-ARZ — 2
Washington, DC 20310

US Army Materiel Systems Analysis Activity
ATTN: DRXSY-MP — 1
Aberdeen Proving Ground, MD 21005

IIT Research Institute
ATTN: GACIAC — 1
10 West 35th Street
Chicago, IL 60616

Chief
Bureau of Naval Weapons
Department of the Navy 1
Washington, DC 20390

Chief
Bureau of Ships
Department of the Navy 1
Washington, DC 20315

Naval Research Laboratory
ATTN: Dr. M. M. Drafft
Code 8430 1
Washington, DC 20375

Commander
Wright Air Development Division
ATTN: ASRC 1
Wright-Patterson Air Force Base, OH 45433

Director
Air Force Materiel Laboratory
ATTN: AFML-DO-Library 1
Wright-Patterson Air Force Base, OH 45433

Director
Army Materials and Mechanics Research Center
ATTN: DRXMR-PL 1
-MT, Mr. Farrow 1
Watertown, MA 02172

Commander
White Sands Missile Range
ATTN: STEWS-AD-L 1
White Sands Missile Range, NM 88002

Jet Propulsion Laboratory
California Institute of Technology
ATTN: Library/Acquisitions 111-113 1
4800 Oak Grove Drive
Pasadena, CA 91103

Sandia Laboratories
ATTN: Library 1
P. O. Box 969
Livermore, CA 94550

Commander
US Army Air Defense School
ATTN: ATSA-CD-MM 1
Fort Bliss, TX 79916

Armament Development and Test Center
ATTN: DLDSL 1
Eglin Air Force Base, FL 32542

University of California
Los Alamos Scientific Laboratory
ATTN: Reports Library 1
P. O. Box 1663
Los Alamos, NM 87545

Commander
US Army Materiel Development and Readiness Command
ATTN: DRCRD 1
DRCDL 1
5001 Eisenhower Avenue
Alexandria, VA 22333

Director
Defense Advanced Research Projects Agency 1
1400 Wilson Boulevard
Arlington, VA 22209

DRSMI-LP, Mr. Voigt 1
-R 1
-RL, Mr. Comus 1
-RLA, Mr. Pettey 1
-RLA 1
Mr. Schaeffel 50
-RPT (Reference Copy) 1
(Record Copy) 1
-RPR 15

END

DATE
FILMED

4-81

DTIC